Robotica (2001) volume 19, pp. 163–176. Printed in the United Kingdom © 2001 Cambridge University Press

Sagittal gait of a biped robot during the single support phase. Part 1: passive motion*

Mostafa Rostami and Guy Bessonnet

Laboratoire de Méchanique des Solides – UMR 6610 CNRS, Université de Poitiers, SP2MI, Teleport 2, Bd Marie et Pierre Curie, BP 30179, 86962 Futuroscope Chasseneuil Cedex (France). E-mail: Guy.Bessonnet@lms.univ-poitiers.fr

(Received in Final Form: July 26, 2000)

SUMMARY

It has been shown that compass-like bipeds can walk passively by gravity-induced motion. Similarly, it has been stated that the unipodal phase of human gait may be regarded as a passive motion. This paper is aimed at determining precisely to what extent the swing phase of human-like walking can be considered as a non-actuated motion. More specifically, a method is developed that makes it possible to adjust initial conditions, step length and walk speed, as well as mass and inertia distribution of a bipedal robot, in order to generate a passive swing motion. The approach is demonstrated by using a 7-link planar biped. Numerical simulations show that purely passive unipodal transferring cannot be fully satisfactory. This approach is further considered in Part 2 of the paper which consists in computing optimal actuating joint torques to create perfectly feasible motions.

KEYWORDS: Sagittal gait; Single support phase; Bipedal robot; Dynamics of walking; Passive motion.

1. INTRODUCTION

The interest of researchers for legged locomotion has been constantly increasing in both areas of biomechanics and robotics. At first, the need for a better analysis of human gait has resulted in designing computerized motion analysis systems. On this basis, experimental reconstruction of motion kinematics together with ground reaction-force measurement make it possible to determine, using inverse dynamics, the joint actuating torques, as well as the mechanical energy expenditure involved during the observed motion. Next, another interesting and complementary approach consists in simulating human gait by using a direct dynamic model, and minimizing a performance index in order to generate an optimal gait step.[1,2] Such attempts to identify some generating principles of gait are based on the minimization of actuating forces or energy consumption. The latter approach has been used as well to generate gait cycles of bipedal robots. Obtaining reference gait patterns will help to drive and control the robot.

In other respects, the bipedal gait has drawn researchers attention to some of its qualitative aspects such as particularly the intrinsic dynamic behaviour of the biped. On this subject, it clearly appears that the biped transferring from one foot to the other depends quite closely on gravity together with the inertia of locomotion limbs. The gravity-inertia coupling effect on bipedal gait is especially at stake during the single-support phase which represents about 80% of the gait cycle.[3]

During this swing motion, the biped can perform seemingly as a multi-link, inverted pendulum. As we will see in what follows, this passive aspect of gait has been tackled in various ways.

Papers dealing with bipedal locomotion are mainly devoted to the swing motion which is, as we mentioned just above, the main phase of gait owing to its large amplitude, and also its great instability. It is the same choice we propose here. The study is organized in two papers: The first one deals with the existence of passive pendular gaits during the swing phase of walking. The companion paper is devoted to dynamic optimization of biped locomotion during the same single-support phase.

In part 1 of the two parts paper we want to examine to what extent the swing phase of human-like gait may be described as a passive motion. This question has received satisfactory answers for compass-like bipeds, but has only been taken into consideration without being really solved for the case of human-like locomotion.

The concept of passive gait has been especially developed by McGeer.[4,5] In reference [4], the author studies the ability of a compass like structure to perform a passive sagittal gait. The dynamic behaviour of such a simple system is not obvious. McGeer established that this biped can walk down a slope by gravity-induced passive motions. This idea is pursued in references [6 & 7] where the existence of passive walking on a sloping floor is thoroughly established.

McGeer also studied the passive gait of a biped provided with legs flexing at knee joints.[5] This four-link mechanical system is designed in such a way the knees can passively lock and unlock in order that the biped does not collapse. A point mass at the hip is used to represent a torso.

Roughly speaking, we can say that the passive motion during the unipodal phase is the result of a good combination between initial conditions and gravity-inertia coupling effect, while the impact at heel-touch is expected to restore, at start of the next step, new initial conditions identical or closely related to the previous ones.

Now, one can ask if such a passive dynamic behaviour during the swing phase can be reproduced with more complex bipeds such as human-like walking machines. A response to this question can be partly found in Pratt and

* Part 2 to appear in the next issue of *Robotica*.

https://doi.org/10.1017/S0263574700003027 Published online by Cambridge University Press

Pratt.[8,9] The authors generate gait patterns of planar and 3D bipeds which combine free knee joint with a compliant ankle of the swing leg considered as passive. In this way, the motion benefits from natural dynamics of the biped. In other respects, with regard to human gait, McMahon in reference 10 (see also references 11 & 12) observes that electromyographic analysis shows there is very little activity of swing-leg muscles during the unipodal phase. He concludes that the swing phase may be considered as the passive motion of a jointed pendulum. This model implies that the bipodal phase creates initial conditions of the swing in order that the pendular transferring of the biped may be considered as a feasible motion. That is to say, the swing leg must only flex forwards, its foot must not collide with the ground, and heel-touch must occur at the right place with a moderate impact velocity. This is the problem we intend to solve in this paper. We deal with a 7-link planar biped comprising a trunk. The feet perform functionally as human ones. The method we propose is quite general and can be easily extended to any pendular motion for transferring passively a multibody mechanical system from a given initial configuration to a prescribed final one.

The technique developed can be used too as a design tool to optimally adjust some geometric dimensions and inertia distribution of links in order to improve the ability of the mechanical system to generate the expected passive dynamic behaviour.

This work has been achieved within the framework of a research joint project presented in reference [13], and which consists in designing and realizing an anthropomorphic biped robot aimed at reproducing human-like gaits (see also references [14 & 15]).

2. DYNAMIC MODEL OF THE PASSIVE BIPED

In this section we present the assumptions which define the problem to be dealt with. The result is the study of a planar movement with 3 degrees of freedom (dof) of a 4-link mechanical system.

We consider a sagittal model of an anthropomorphic biped, the minimum criterion for anthropomorphic characteristics being the presence of knee joints.

The basic model we consider has 7 links including feet, legs, thighs and a trunk (see Figure 1). Such a planar system is provided with six joints: two ankles, two knees and two coaxial joints at the hip.

Such a model makes it possible to simulate the human gait in the sagittal plane when the sway motion (frontal rotation of the pelvis) is not very important. The study of passive swing during the single support phase requires to reduce the mobility of the biped. The following assumptions correspond as much as possible to human walking:

(i) The foot of the stance leg remains flat on the ground during the swing phase. Furthermore, in order to avoid the sole could be regarded as stuck on the ground, the normal ground-reaction forces must remain positive throughout the movement. This constraint simply expresses the unilaterality of contact forces exerted by the ground on the foot.

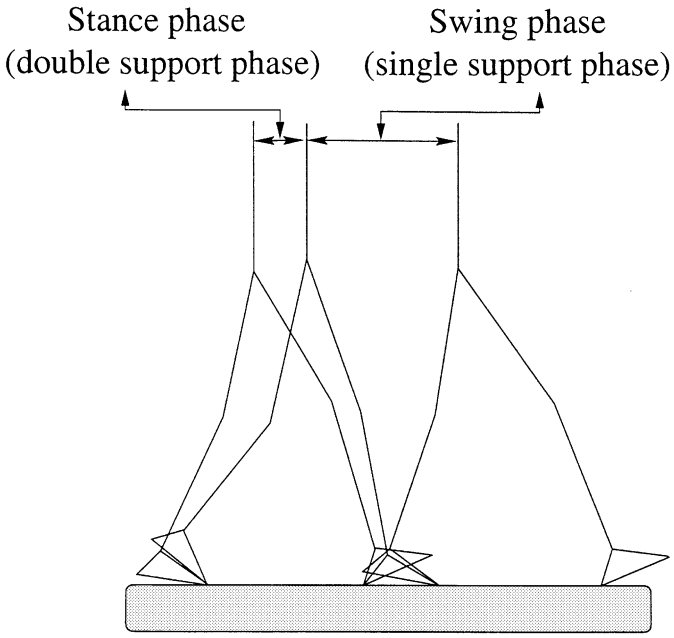


Fig. 1. Human walking in the sagittal plane.

(ii) The trunk keeps a constant tilt. Since the trunk is not stable, its articulation with the stance leg must remain active. In the numerical applications, we shall notice that the joint torque required to hold the trunk in position is not very great. This remark agrees with the fact that during the swing phase of human gait, the variation of the absolute angle of the trunk during the swing phase is small and can be neglected. Because of the presence of this powered joint, the movement of the biped could not be regarded as purely conservative but only as quasi-conservative.

(iii) Observation of human gait shows that the ankle rotation of the swing foot is quite small. In accordance with this fact, we assume that the ankle of the swing leg of the passive biped is locked during the swing motion.

(iv) The knee of the stance leg must be considered stiff in the pendular model in order to avoid the biped's collapses. The stance leg is assumed to be in full extension.

Through the previous assumptions the biped is expected to perform as an inverted pendulum (the stiff stance leg) supporting a double pendulum (the swing leg) and a fourth body (the trunk) whose absolute pitch is specified. One can consider the kinematic tree structure of this multibody system to be the simple kinematic chain

$$L_1 \leftrightarrow L_4 \leftrightarrow L_2 \leftrightarrow L_3$$

The constant pitch of the trunk is defined by the angle $\alpha = (X_0, X_4)$, and the relative angle of the foot of the swing leg is shown by the constant angle $\beta = (X_3, X_3')$ (Figure 2).

The description of the movement is realized through the introduction of a configuration reduced to three independent joint coordinates describing the rotations of the passive joints: ankle of the support leg, hip and knee of the swing leg. The movement being plane, it is judicious to use absolute joint coordinates defined as

https://doi.org/10.1017/S0263574700003027 Published online by Cambridge University Press

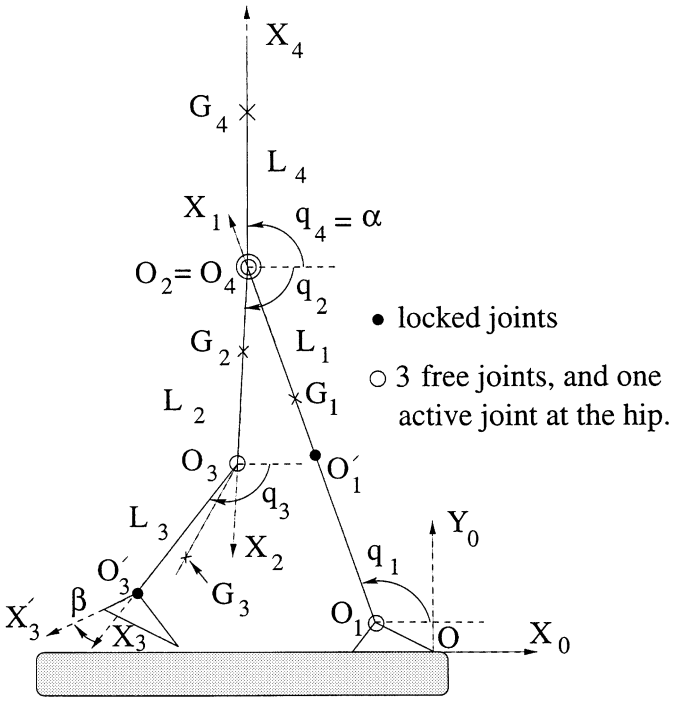


Fig. 2. Passive model with 4 links, 3 dof, and stiff stance leg.

$$q_i = (X_0, X_i), \quad i = 1, 2, 3$$

So, the position vector is given by $\mathbf{q} = (q_1, q_2, q_3)^T$.

The forces acting on the mechanical system are due to gravity together with the active joint torque T_{14} exerted by L_1 on L_4 to maintain the pitch of the trunk constant during the movement. The configuration with three independent parameters leads to three independent motion equations in which the unknown torque T_{14} must be expressed as a function of the type T_{14} ($\mathbf{q}$, $\dot{\mathbf{q}}$, $\ddot{\mathbf{q}}$) depending on $\mathbf{q}$, and its first and second time derivative $\dot{\mathbf{q}}$, $\ddot{\mathbf{q}}$. This formulation is derived in Appendix 1. Formally, we shall represent the three independent equations of motion as

$$\mathcal{L}_i(\mathbf{q}, \dot{\mathbf{q}}, \ddot{\mathbf{q}}) = 0, \quad i = 1,\ 2,\ 3 \tag{1}$$

3. CONSTRAINTS

Two types of conditions to fulfill during the swing phase can be distinguished according to whether they are instantaneous or permanent. The first type includes initial and final constraints on the contacts between the transferred foot and the ground. They must make it possible to respect the step length so as to generate a cyclic walking. They also comprise non-sliding conditions at the moments of toeing-off and heel-touch. Constraints of the second type will be designed to prevent counter-flexion of the swinging leg, and as well to avoid contact of the foot with the ground or an obstacle during the swing motion.

3.1 Initial constraints

At initial time of the swing phase (moment of toeing-off), the only imposed conditions relate to the position and the velocity of the ball of the swing foot, which is represented by the point of contact D^i in Figure 3. We have two constraints on the position of the point D^i: a first one expressing the contact between the foot and the ground, and a second one representing the step length.

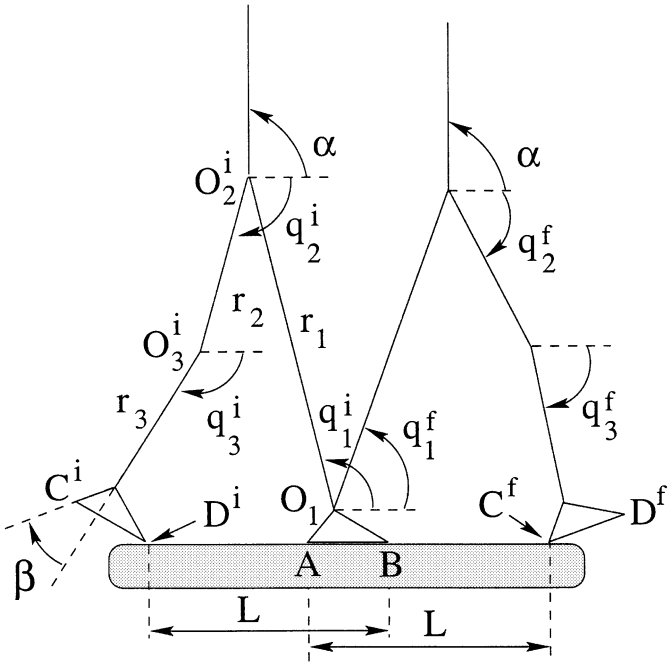


Fig. 3. Configurations of the biped at toe-off and heel-touch.

These two constraints can be written in the form:

$$\begin{aligned} OD^i \cdot Y_0 &= 0\,, \\ OD^i \cdot X_0 + L &= 0\,, \end{aligned} \tag{2}$$

where O = B and L is the step length (see Figure 3) which must be determined.

We must also specify two constraints on the velocity of the point D^i at the initial time. At this moment, the foot can have an angular velocity about D^i, but its linear velocity must be equal to zero. This condition can be written as:

$$\begin{aligned} V(D^i) \cdot X_0 &= 0\,, \\ V(D^i) \cdot Y_0 &= 0\,. \end{aligned} \tag{3}$$

Initial constraints (2) and (3) can be formally represented by functions g_j such as:

$$g_j(\mathbf{q}^i, \dot{\mathbf{q}}^i, \beta) = 0\,, \quad j = 1,\ \ldots,\ 4 \tag{4}$$

where $\mathbf{q}^i$ (resp. $\dot{\mathbf{q}}^i$) stands for the initial value of the joint position (resp. velocity) vector at toe-off time.

3.1.1 Singularity of the model. For each set of values of the three parameters ${q_1}^i$, β and L we have two possible different configurations of the swing leg (Figure 4). We can distinguish these two configurations by the position of the heel: "heel up" when the leg profile $O_2^i O_3^i D^i$ is flexed forwards at point O_3^i, and "heel down" when $O_2^i {O'}_3^i D^i$ is flexed backwards at point ${O'}_3^i$ (see Figure 4).

For fixed values of the two parameters β and L (Figure 3) when the angle ${q_1}^i$ decreases, these two configurations get closer. There is a limiting value ${q_1}^s$ of ${q_1}^i$ for which there is superposition. In that case, the knee of the swing leg is located on the straight line $O_2^i D^i$ (Figure 4). This configuration is singular; for a non-zero value of $\dot{q}_1^i$, joint velocities $\dot{q}_2^i$

https://doi.org/10.1017/S0263574700003027 Published online by Cambridge University Press

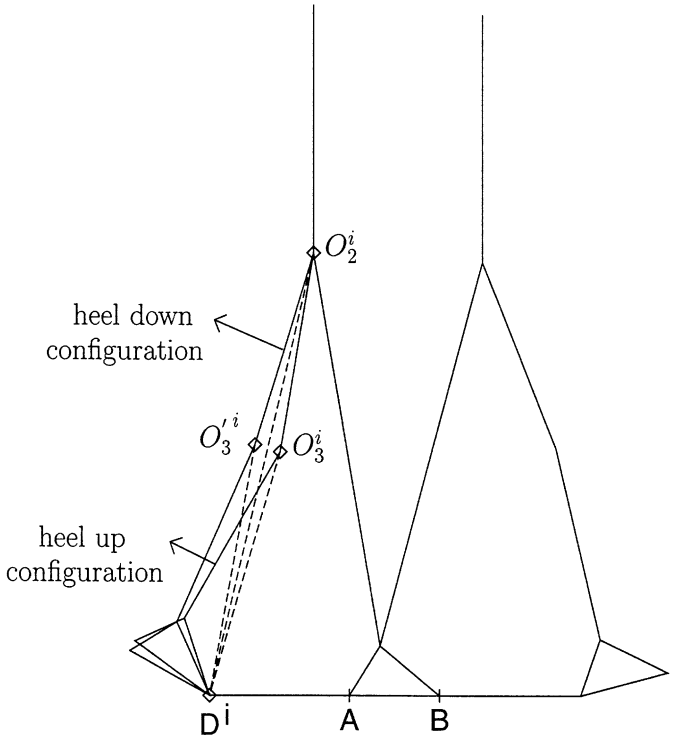


Fig. 4. Configurations "heel up" and "heel down" at initial time of the swing phase.

and $\dot{q}_3^i$ tend towards infinity when the angle $q_1{}^i$ tends towards $q_1{}^s$.

By using the equiprojectivity property of velocity vectors of each link, we can construct the velocity vector of the knee-joint center in the two configurations "heel down" and "heel up" (see Figure 5). We can note that these two vectors $\mathbf{V}_{O_3'^i}$ and $\mathbf{V}_{O_3^i}$ have greater magnitude than $\mathbf{V}_{O_2^i}$ (hip velocity vector). Moreover, these two vectors have almost opposite directions.

For the upper position of the heel, the knee velocity-vector is directed in the opposite direction of walking. This initial configuration can produce a counter-flexion of the leg, and, therefore, is inappropriate to generate a passive motion of an anthropomorphic type. For this reason, the simulations presented in what follows, are limited to the case of the heel in lower position. Nevertheless, in the companion paper (Part 2), in which all joints are considered as active, we will carry out a search for optimal movements by using one or the other of these two initial configurations. We will note that the optimal motions starting with the knee in lower position are closer to human movements and less energy consuming than motions optimized in the other case.

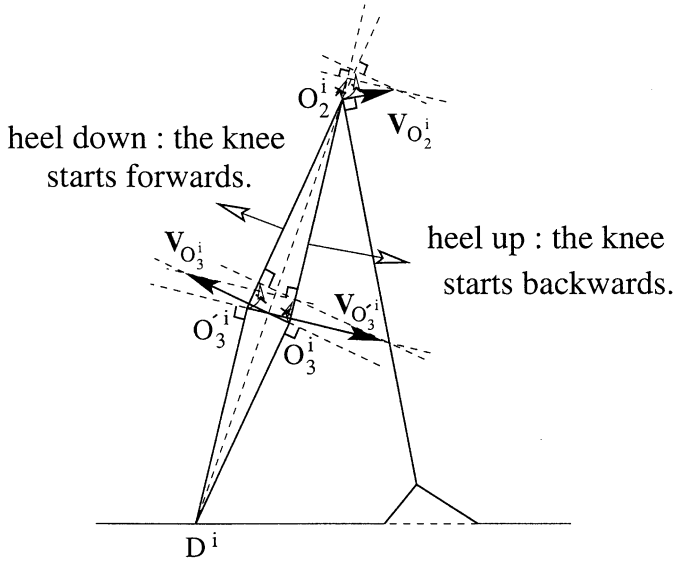


Fig. 5. Construction of vectors $\mathrm{V}_{O'^i_3}$ and $\mathrm{V}_{O^i_3}$ by using the equiprojectivity property.

3.2 Final constraints

At the end of the swing phase, as in the previous case, we have four constraints to formulate on the position and velocity of the point C^f (Figure 3). Two constraints define the position of this point: one to ensure that the heel is in contact with the ground and the other to respect the step length, namely

$$\begin{aligned} OC^f \cdot Y_0 &= e_1 \ , \\ OC^f \cdot X_0 - (L-l) &= e_2 \ , \end{aligned} \tag{5}$$

where e_1 and e_2 represent errors between a reached position and the specified position. "l" is the length of the foot.

In addition, we are seeking for a pendular motion ending with a moderate impact velocity. Thus, we define the two components of the velocity vector of C^f in the form

$$\begin{aligned} V(C^f) \cdot X_0 &= e_3 \ , \\ V(C^f) \cdot Y_0 &= e_4 \ , \end{aligned} \tag{6}$$

where the values e_3 and e_4 must be minimized. In what follows, constraints (5) and (6) will be written as the functions h_j

$$h_j(\mathbf{q}^f, \dot{\mathbf{q}}^f, \beta) = e_j \ , \quad j = 1, \ \ldots \ , \ 4 \tag{7}$$

where the superscript "f" designates values at final time.

3.3 Permanent constraints

Initial and final constraints are not sufficient to ensure that the movement is feasible. We shall consider that a pendular step is not feasible if the swing leg presents a hyper-extension and/or its foot has intermediate contacts with the ground. Figure 6 shows two examples of non-feasible

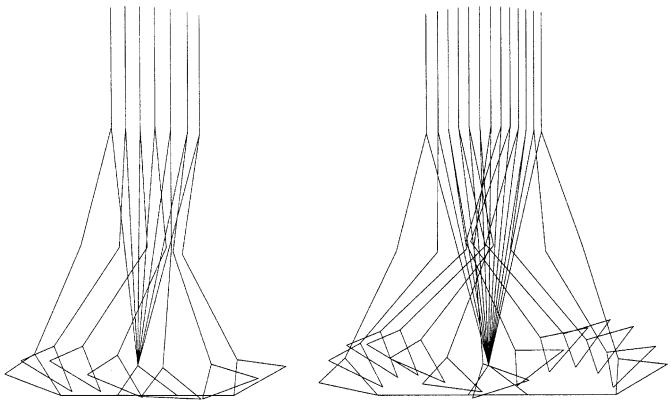


Fig. 6. Non-feasible pendular motions respecting initial and final constraints.

https://doi.org/10.1017/S0263574700003027 Published online by Cambridge University Press

computed movements respecting the initial and final constraints (the first with a counter-flexion and the second with a double change of concavity at the knee).

To prevent counter-flexion of the knee of the swing leg, we specify a constraint of the type:

$$\theta \equiv q_3 - q_2 \leq 0 \tag{8}$$

where θ represents the relative rotation angle of the knee.

We formulate also two additional constraints in order to avoid any contact between the swing foot and the ground. The two end points C and D of the foot (see Figure 3), must satisfy

$$h_C > 0\,, \quad h_D > 0 \tag{9}$$

where h_C and h_D represent the normal distances between end points and the ground.

The constraints (8) and (9) depend on the free joint coordinates q_k, $k \leq 3$. The variations of q_k depend on the mechanical characteristics of the biped together with the selected numerical values for the initial state, that is ($\mathbf{q}^i$, $\dot{\mathbf{q}}^i$, β). The stated problem consist in choosing these values in such a way that the generated motion respects all the constraints. In order to satisfy these constraints of inequality type, we use a penalty method presented in the sub-section 4.3.

4. A MINIMIZATION PROBLEM

We want to generate a passive swing-motion of the biped satisfying the set of constraints (4), (7), (8) and (9) formulated in the previous section. The approach we propose roughly consists in finding initial conditions $\mathbf{q}^i$ and $\dot{\mathbf{q}}^i$ defining the joint positions and giving the momentum which will allow the biped to be transferred passively close to a final position satisfying the constraints (5) and (6) with small errors e_1 and e_2 and moderate impact velocities e_3 and e_4.

4.1 Objective function

In fact, we are seeking the best conditions allowing the residual values e_i ($i \leq 4$) of functions h_i in (7) to be minimized.

One can think that the success of the adjustment process not only will depend on the six initial parameters q_j^i, $\dot{q}_j^i$ (j = 1, 2, 3), but will depend as well on the travelling time T. One can add to the previous parameters, the determination of the angle β which defines an initial angular position of the foot at ankle (Figure 2). Therefore, we introduce the eight following control parameters put together into the vector $\mathbf{x}$ as

$$\mathbf{x} = (x_1, \ldots, x_6, x_7, x_8)^T \equiv (q_1^i, q_2^i, q_3^i, \dot{q}_1^i, \dot{q}_2^i, \dot{q}_3^i, \beta, T)^T \tag{10}$$

Consequently, we regard the final state ($\mathbf{q}^f$, $\dot{\mathbf{q}}^f$) of the mechanical system as depending on $\mathbf{x}$. Thus, we reconsider the final constraints h_j in (7) to be the new functions h_j^* in $\mathbf{x}$ such as:

$$h_j^*(\mathbf{x}) \equiv h_j(\mathbf{q}^f(\mathbf{x}),\ \dot{\mathbf{q}}^f(\mathbf{x}),\ x_7) = e_j\,, \quad j \leq 4 \tag{11}$$

Now, we can define the quadratic function F^* in $\mathbf{x}$ of the h_j^* as:

$$F^*(\mathbf{x}) = \frac{1}{2}\,[\mu \times (h_1^{*2}(\mathbf{x}) + h_2^{*2}(\mathbf{x})) + (1-\mu) \times (h_3^{*2}(\mathbf{x}) + h_4^{*2}(\mathbf{x}))] \tag{12}$$

Our objective is to minimize this function while respecting the initial constraints defined by the formulas (4). This problem is a nonlinear optimization problem with equality constraints. The factor μ is a weighting coefficient which acts in the following way:

(i) If μ = 1, the error on the position only is minimized. In this case, we only seek to reach the symmetrical point without trying to minimize the impact velocity.

(ii) If μ = 0, only the impact velocity is minimized. In this case, the error on the position is not subjected to any condition.

(iii) If $0 < \mu < 1$, the factor μ can be used as a "weighting factor" making possible to balance the minimization between error in position, and components of the impact velocity or, on the contrary, to privilege the minimizing effect on one or the other quantity.

4.2 Alternative formulation of an unconstrained problem

It is possible to introduce some simplifications in the problem. In the vector $\mathbf{x}$, the parameters q_1^i, q_2^i, q_3^i are not independent because of the two initial constraints (2) on the position of the point D^i (Figure 3). For example, for each value of q_1^i we can determine the values of q_2^i and q_3^i by using these two initial constraints. In this case, we reduce to six the number of parameters to be determined by the optimization process. Moreover, the initial constraints on the position will be automatically respected. We can use the same approach for the three parameters $\dot{q}_1^i$, $\dot{q}_2^i$ and $\dot{q}_3^i$; for each value of $\dot{q}_1^i$, we can determine the values of $\dot{q}_2^i$ and $\dot{q}_3^i$ by using the initial constraints (3) on the velocity of the point D^i (Figure 3). Thus, we reduce to 4 the number of control parameters, the 4 initial constraints in (4) being automatically respected. By this way, the problem can be recast into an unconstrained minimization problem.

4.3 Inequality constraints and penalized objective function

With the approach presented above, the initial constraints are respected perfectly while the final constraints are also satisfied. But, to generate a feasible motion, it may be necessary to respect additional constraints throughout the movement, as defined in subsection 3.3. As the motion is passive, we do not have any direct control on the joint variables. Nevertheless, it is possible to take into account such permanent constraints by injecting them in a certain manner into the objective function F^* (formula (12)). We define this additional term in such a way that, when the algorithm minimizes it, the corresponding constraint is respected at best. For example, if we want to avoid counter-flexion at the knee of the swing leg, it will be necessary for the relative rotation angle at knee to remain negative during the swing phase as indicated by (8). When this constraint is not respected, there is a part of the movement during which this angle becomes positive. Then, we define:

$$t \in [0, T],\ \ \theta^+(t) = Max(0, \theta(t))$$

https://doi.org/10.1017/S0263574700003027 Published online by Cambridge University Press

where the function θ^+ takes the zero value when the inequality constraint $\theta(t) \leq 0$ is respected, and the value $\theta(t)$ when this constraint is infringed.

The penalty method we use consists in minimizing the positive function θ^+ by adding its quadratic value to the objective function F^*. In order to intensify the minimizing effect on θ^+, this additional term is multiplied by a penalty factor r which is intended to tend towards infinity. But, it is well known that for increasing values of r, the numerical conditioning of the minimization problem deteriorates. A simple means to avoid this difficulty consists in substituting the function

$$\theta_b^+ = Max(0,\, \theta(t) + b)\,, \quad b > 0$$

for θ^+, where b is a correcting value to be chosen by the solving algorithm. In this way, the effective reduction of the constraint to zero is obtained for a moderate value of r.

Now, we must notice that the evolution of the angle θ depends, through the vector $\mathbf{q}$ of joint coordinates (cf. (8)), on the values of initial parameters put together in $\mathbf{x}$ (see (10)). Consequently, θ and θ_b^+ present a dependence of the type $\theta(\mathbf{q}(\mathbf{x}, t))$, $\theta_b^+(\mathbf{q}(\mathbf{x}, t))$. As a result, we obtain the more explicit expression for θ_b^+

$$\theta_b^+(\mathbf{q}(\mathbf{x}, t)) = Max(0,\, \theta(\mathbf{q}(\mathbf{x}, t)) + b) \tag{13}$$

Figure 7 shows, as an example, possible variations of the angle θ, and the correlative variations of θ_b^+.

Then, the function θ_b^+ is introduced into the objective function in the following way:

$$F(\mathbf{x}) = F^*(\mathbf{x}) + rG(\mathbf{x}) \equiv F^*(\mathbf{x}) + F_r(\mathbf{x}) \tag{14}$$

where

$$G(\mathbf{x}) = \int_0^T [\theta_b^+(\mathbf{q}(\mathbf{x}, t))]^2\, dt \tag{15}$$

Integrating the motion equations (1) for any given value of $\mathbf{x}$, yields the corresponding movement of the biped, that is $t \rightarrow \mathbf{q}(\mathbf{x}, t)$. At final time $t = T$, one obtains from this result, the final values $\mathbf{q}^f$ and $\dot{\mathbf{q}}^f$ of $\mathbf{q}$ and $\dot{\mathbf{q}}$. Then, it is possible to compute $F^*(\mathbf{x})$ through (11) and (12). After that, considering (8) and (13), and computing the integral in (15) yields the numerical value of $F_r(\mathbf{x})$ in (14). Thus, for any selected value of the vector $\mathbf{x}$, we obtain the corresponding value of $F(\mathbf{x})$.

Now, we intend to find some value of $\mathbf{x}$ minimizing the function $F(\mathbf{x})$.

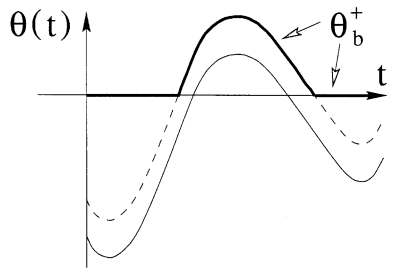


Fig. 7. Functions θ and θ_b^+.

4.4 Necessary conditions of optimality

We consider the problem which consists in determining the unknown vector $\mathbf{x}$ satisfying the constraints $g_j(\mathbf{x}) = 0$ (see (4)) and which minimizes the penalized objective function $F(\mathbf{x})$ defined in (14). This is a nonlinear minimization problem with equality constraints.

Necessary conditions for the existence of a solution are formulated in many optimization text-books (see, for example references [16, 17]. Introducing Lagrange's multipliers λ_j, they can be written as

$$\begin{cases} \dfrac{\partial F}{\partial x_i} + \sum_{j=1}^{4} \lambda_j \dfrac{\partial g_j}{\partial x_i} = 0\,, \quad i = 1,\, \ldots,\, 8 \\ g_j(\mathbf{x}) = 0\,, \quad j = 1,\, \ldots,\, 4 \end{cases} \tag{16}$$

where

$$\frac{\partial F}{\partial x_i} = \sum_{j=1}^{2} \left[\mu h_j^*(\mathbf{x}) \frac{\partial h_j^*}{\partial x_i} + (1-\mu) h_{2+j}^*(\mathbf{x}) \frac{\partial h_{2+j}^*}{\partial x_i} \right] + \frac{\partial F_r}{\partial x_i} \tag{17}$$

All the derivatives $\partial g_j / \partial x_i$ in (16) can be formulated explicitly. They can also be computed by numerical differentiations.

Firstly, we can notice that g does not depend on T, i.e. $\partial g(\mathbf{x})/\partial T = 0$. Secondly, g_1 and g_2 depend on joint coordinates only ($q_i \equiv x_i$, $i \leq 3$). To carry out numerical differentiation, we consider small increases $\delta \mathbf{x}_k$ of the x_k's so as to formulate the approximate derivative

$$\frac{\partial g_j}{\partial x_k} \cong \frac{[g_j(\mathbf{x} + \delta \mathbf{x}^{(k)}) - g_j(\mathbf{x} - \delta \mathbf{x}^{(k)})]}{2\delta x_k} \tag{18}$$

where the only non-zero component in

$$\delta \mathbf{x}^{(k)} = (0_1, \ldots, 0_{k-1}, \delta x_k, \ldots, 0_8)$$

is the k^{th} one.

The derivatives of $h_j^*(\mathbf{x})$ in (17) are more tricky to compute owing to the fact that these functions depend on x_k's through the final values of $\mathbf{q}$ and $\dot{\mathbf{q}}$ (see (11)).

As for the functions g_j's we make use of a formula similar to (18), namely

$$j \leq 4,\ k \leq 8,\ \frac{\partial h_j^*}{\partial x_k} \cong \frac{h_j^*(\mathbf{x} + \delta \mathbf{x}^{(k)}) - h_j^*(\mathbf{x} - \delta \mathbf{x}^{(k)})}{2\delta x_k} \tag{19}$$

The computation of h_j^*'s appearing in the right hand member requires to distinguish both following cases.

(i) **Case** $k \leq 7$

The transfer time T ($T \equiv x_8$) being fixed, the perturbation δx_k represents a small variation of the k^{th} initial data in (10), represented by q_j^i or $\dot{q}_j^i$ ($j \leq 3$), or β for $k = 7$. Integration of the motion equations (1) on the time interval $[0, T]$ yields the corresponding final values $\mathbf{q}^f$ and $\dot{\mathbf{q}}^f$ which allow the h_j^*'s to be computed in (11). Consequently, two successive integrations carried out with initial conditions as $\mathbf{x} + \delta \mathbf{x}^{(k)}$ and $\mathbf{x} - \delta \mathbf{x}^{(k)}$ lead to the computation of the h_j^* terms in (19). Repeating this operation for k varying from one to seven, one complete the numerical differentiation of all h_j^* with respect to x_k for $k \leq 7$.

https://doi.org/10.1017/S0263574700003027 Published online by Cambridge University Press

(ii) **Case** $k = 8$ ($x_8 \equiv T$)

In this case δx_8 represents a perturbation of the transfer time T. With fixed values of x_k's, $k \leq 7$, two successive integrations of motion equations on the time intervals $[0, T + \delta T]$ and $[0, T - \delta T]$ yield, as above, the corresponding final values $\mathbf{q}^f$ and $\dot{\mathbf{q}}^f$ which allow the $h_j^*(\mathbf{x} + \delta\mathbf{x}^{(8)})$ and $h_j^*(\mathbf{x} - \delta\mathbf{x}^{(8)})$ in (19) to be computed through (11). The numerical values of all h_j^* derivatives with respect to T result immediately from (19).

The derivatives of the penalty function G in (15) are also required. As previously, we make use of the centered derivation formula

$$k \leq 8, \frac{\partial G}{\partial x_k} \cong \frac{G(\mathbf{x} + \delta\mathbf{x}^{(k)}) - G(\mathbf{x} - \delta\mathbf{x}^{(k)})}{2\delta x_k} \qquad (20)$$

For each $k \leq 7$, two integrations of motions equations starting with $\mathbf{x} + \delta\mathbf{x}^{(k)}$ and $\mathbf{x} - \delta\mathbf{x}^{(k)}$ as initial values, yields the functions $t \rightarrow \mathbf{q}(\mathbf{x} + \delta\mathbf{x}^{(k)}, t)$, $t \rightarrow \mathbf{q}(\mathbf{x} - \delta\mathbf{x}^{(k)}, t)$. With every one of these results, we compute successively θ_b^+ in (14), G in (16), and finally the derivatives of G in (20).

For $k = 8$, x_8 represents the motion time T. One gets directly

$$\frac{\partial G}{\partial x_8} \equiv \frac{\partial G}{\partial T} = [\theta_b^+(\mathbf{x}, T)]^2. \qquad (21)$$

All previous derivatives are required to solve efficiently the minimization problem.

4.5 Solving technique

We solved the stated problem by using the routine E04UCF of the NAG *Fortran* Library. This computing code is designed to minimize an arbitrary smooth function depending on variables subjected to constraints which may include simple bounds on the variables, linear constraints and smooth nonlinear constraints. The user must provide, as far as possible, the first partial derivatives of the objective function and constraints.

This routine uses a sequential quadratic programming algorithm in which the search direction is the solution of a quadratic programming problem.

For detailed information about such optimization techniques, the reader may refer to textbooks such as Gill *et al.*[18] or Fletcher.[19]

5. FREEING THE MASS DISTRIBUTION

The free motion of a passive locomotion system is the effect of interaction between gravity and inertia of its links. Therefore, one can attempt to adjust the mass distribution of the biped in order to improve its passive dynamic behaviour.

We assume that the geometric dimensions of the kinematic structure together with the total mass of the biped are fixed. On that basis, we intend to evaluate, within some limits, the best mass distribution for each link allowing the biped to improve its passive walk.

We develop this approach on the basis of two simple models: The first one is made up of point masses; in the second model which is more realistic, the links are assumed to be truncated cones with adjustable geometry.

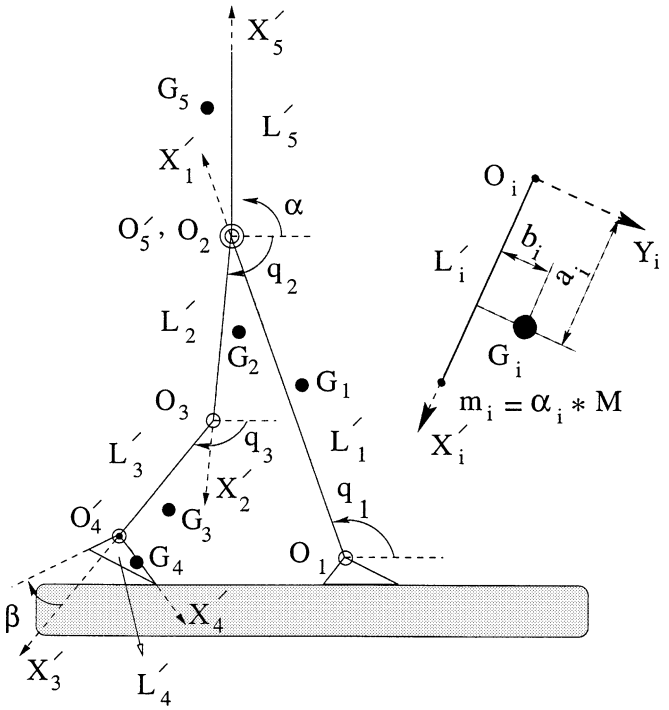


Fig. 8. Model with concentrated masses.

5.1 Links with concentrated masses

The links represented by L'_i, $i \leq 5$ (Figure 8) are assumed to have concentrated masses located at G_i. The parameters a_i and b_i are the local coordinates of the center of gravity G_i of each link L'_i.

Let α_i be the ratio of mass of the link L'_i with respect to the total mass M of the biped. We use the values of the parameters a_j, b_j and α_j = 2, 3, to determine the mass and the position of the center of gravity of the stance leg in such a way that the two legs may have the same inertia characteristics.

In this way, we add 12 unknown parameters (a_i, b_i and α_i for i = 2, . . . , 5) to the previous minimization problem. Therefore, we have 20 parameters to determine in the vector

$$\mathbf{x} = (q_1^i, q_2^i, q_3^i, \dot{q}_1^i, \dot{q}_2^i, \dot{q}_3^i, \beta, T, (a_2, b_2, \alpha_2), \ldots, (a_5, b_5, \alpha_5)) \qquad (22)$$

where the ratios α_i must satisfy the constraint

$$2 \times (\alpha_2 + \alpha_3 + \alpha_4) + \alpha_5 = 1\,, \qquad (23)$$

showing that the total mass of the biped remains constant.

These 12 new variables must be bounded. One can think that with large bounds on these variables, the optimal solution will satisfy all the stated constraints.

5.2 Biped with cone-shaped links

The previous model has two disadvantages:

– it is not a realistic schematization,
– the points G_i may be located rather far from the segmentary axis.

https://doi.org/10.1017/S0263574700003027 Published online by Cambridge University Press

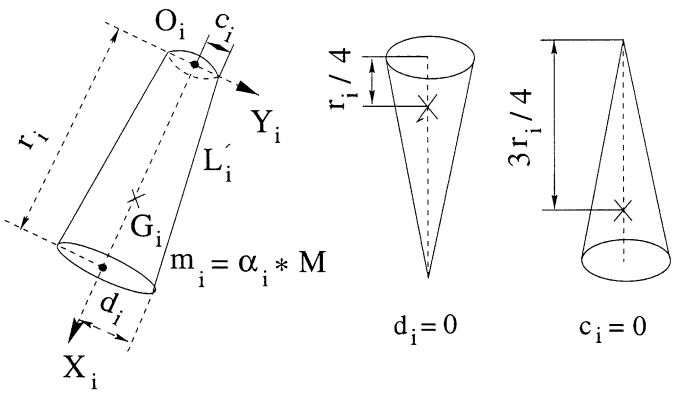


Fig. 9. Model with conical links.

To avoid these consequences, we consider a model with cone-shaped links (Figure 9).

For $i = 2, \ldots, 5$, the geometry of each link L'_i is defined by the three parameters c_i, d_i and r_i. As indicated in Figure 9, the position of the center of inertia of L'_i can vary, according to the values of c_i and d_i, between the lower and upper bounds $\frac{1}{4}r_i$ and $\frac{3}{4}r_i$, where r_i represents the constant length of the segment L'_i. As in the previous case, the mass ratios α_i must satisfy the constraint (23).

Solutions such as $c_i = d_i = 0$, are eliminated by the introduction of bounds and a constraint such as:

$$0 < c_i^{min} < c_i\,, \quad 0 < d_i^{min} < d_i\,, \quad c_i + d_i > \gamma \qquad (24)$$

where c_i^{min}, d_i^{min} and γ are positive values to be specified.

In this case too, we add 12 unknown parameters (c_i, d_i and α_i for $i = 2, \ldots, 5$) in the vector **x**. As previously, **x** groups together 20 unknown quantities to optimize, namely

$$\mathbf{x} = (q_1^i, q_2^i, q_3^i, \dot{q}_1^i, \dot{q}_2^i, \dot{q}_3^i, \beta, T, (c_2, d_2, \alpha_2), \ldots, (c_5, d_5, \alpha_5)) \qquad (25)$$

6. NUMERICAL SIMULATIONS

In this section, we present the results obtained initially with the anthropomorphic mass distribution of the biped "BIP" designed in our laboratory.[13,14,20] Afterwards, we try to improve the dynamic pendular behaviour of the biped by varying its distribution of masses according to both approaches described in the above section. The main mechanical characteristics of the biped BIP are given in Appendix 2.

6.1 Biped with anthropometric mass distribution

We present three results computed with different values of the weighting coefficient μ (see formula (12)).

Example 1

For a value of μ equal to 1, the computed step has the characteristics shown in Table I, while the motion evolution

Table I. Example 1: Step computed characteristics

Time	$\dot{q}_1$	$\dot{q}_2$	$\dot{q}_3$	
t^i	− 1.36	10.25	− 10.26	(rad/s)
t^f	− 2.15	− 5.78	11.89	(rad/s)
L(m)	T(s)	$\bar{v}$(m/s)	v_x(m/s)	v_y(m/s)
0.483	0.33	1.23	5.6	− 2.0

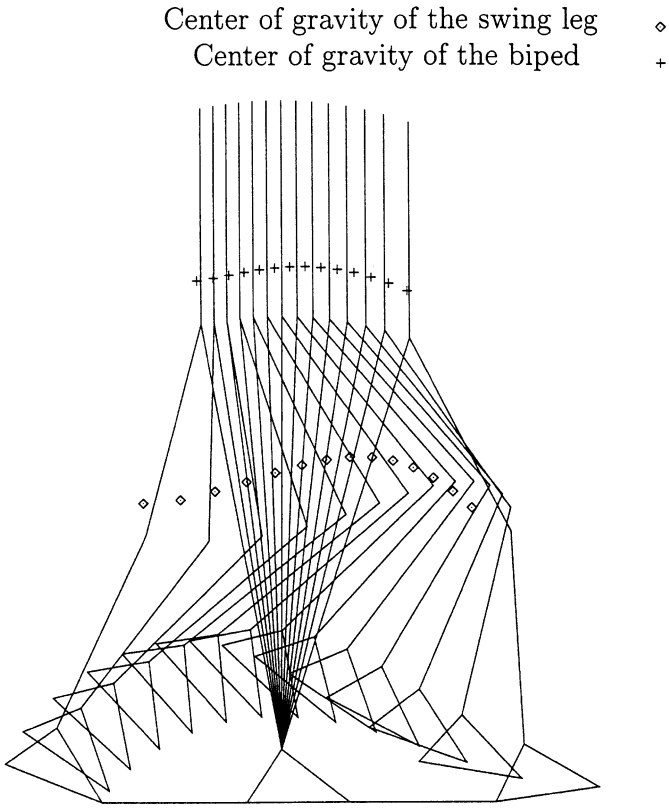


Fig. 10. Example 1: Swing motion of the biped with symmetrical heel-touch.

can be seen in Figure 10. In this case, only the error on the position is minimized. The swing motion shows certain characteristics of the human gait: a quite symmetrical repositioning of the transferred foot, and a forward flexion of the knee of the swing leg. However, the absence of condition on the impact velocity leads to a high value which is much greater than the average speed of the gait. Hence, the computed motion cannot be considered as feasible.

So that the stance foot is not regarded as stuck on the ground, it is necessary that the ground reaction forces remain positive throughout the movement. To verify this condition, we compute the equivalent normal reaction forces applied at the foot end-points *A* and *B* (see Figure 3). It is necessary that these normal components remain positive during the movement. Figure 11 shows that this constraint is respected. But, we can see that the initial impulse produces a significant additional contact force, while at the end of the motion, the normal ground-reaction force is lowered indicating that the biped is collapsing.

Example 2

Now, we decrease the numerical value of μ so as to achieve a simultaneous minimization of the two terms in (12), which define the error on the final position and the components of the impact velocity. The solution which appears in Figure 12 was obtained for $\mu = 0.85$. Both final conditions, symmetrical repositioning of the transferred foot and null impact velocity are perfectly satisfied (see Table II). But the pendular motion shows a double change of concavity of the swing leg which occurs with a collision of the foot with the

https://doi.org/10.1017/S0263574700003027 Published online by Cambridge University Press

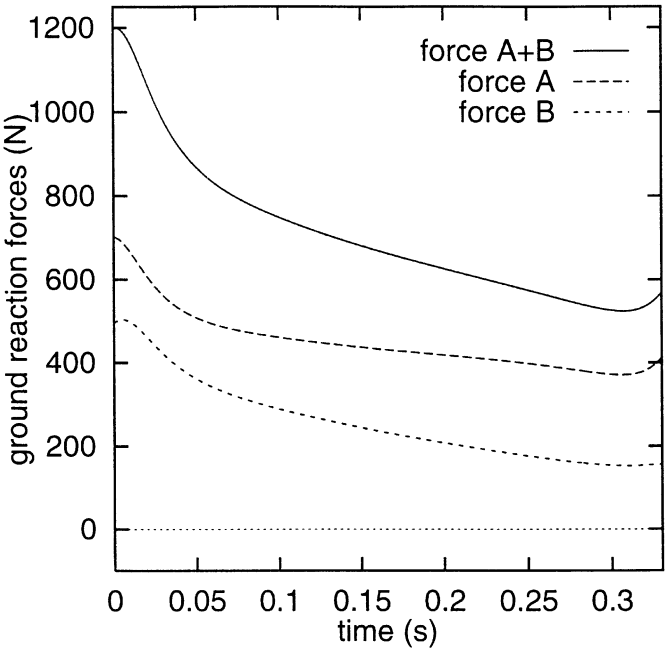


Fig. 11. Example 1: Ground reaction forces.

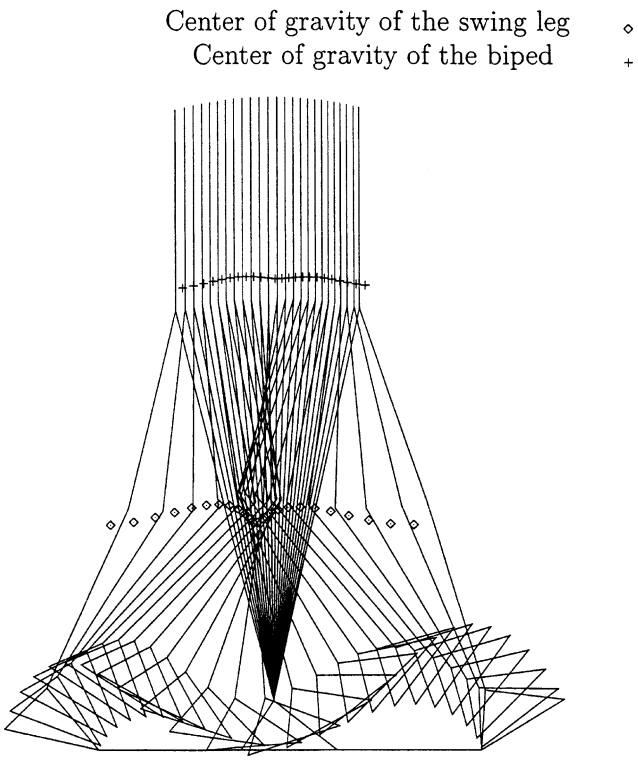


Fig. 12. Example 2: Swing motion with counter-flexion, and impactless symmetrical heel-touch.

Table II. Example 2: Step computed characteristics

Time	$\dot{q}_1$	$\dot{q}_2$	$\dot{q}_3$	
t^i	− 1.2	5.2	− 6.3	(rad/s)
t^f	− 0.96	5.9	− 6.06	(rad/s)
L(m)	T(s)	$\bar{v}$(m/s)	v_x(m/s)	v_y(m/s)
0.5	0.57	0.76	0.0	0.00

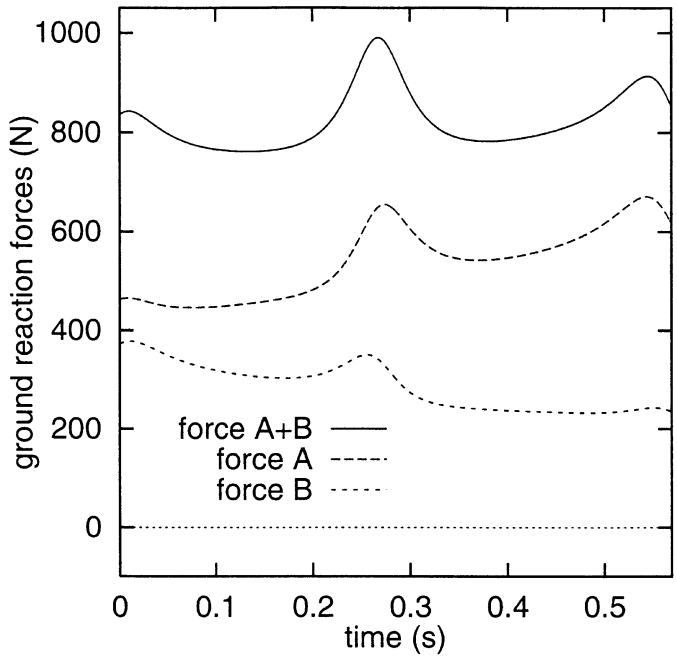


Fig. 13. Example 2: Ground reaction forces.

ground when the leg passes in extension. Such a movement is impracticable.

Comparing the numerical results in Tables I and II, one can notice that for an equivalent step-length the travelling time is noticeably increased. The evolutions of ground reaction forces shown in Figure 13 are quite moderate in comparison with their counterparts of example 1 (Figure 11).

Example 3

In order to prevent the swing leg counter-flexing, and to avoid any intermediate contact between the foot and the ground, we use the penalty technique described in subsection 4.3. In this case, we minimize a penalized function of type (14). The objective is to reach the symmetrical point, without both counter-flexion and intermediate impact, and with a reduced impact velocity. The movement which respects these specifications as much as possible is shown in Figure 14, and its computed characteristics are given in Table III.

In this case, both the step length and the travelling time are reduced. The impact velocity is appreciably reduced as well, compared to that of the first example (see Tables I and III), but it still has a high value. It will be noticed, however, that the motion pattern reflects human walking.

One can observe that the ground reaction forces (Figure 15) are less varying than in both previous cases (Figures 11 and 13). The active torque at hip has moderate variations, as shown in Figure 16.

6.2 Results obtained with concentrated masses

In this case, it is necessary to specify bounds on the 12 additional parameters α_i, a_i, b_i, $i = 2, \ldots, 5$, introduced in (22).

As a first example, we consider enlarged bounds defining the maximum range of admissible values of these new parameters, namely

https://doi.org/10.1017/S0263574700003027 Published online by Cambridge University Press

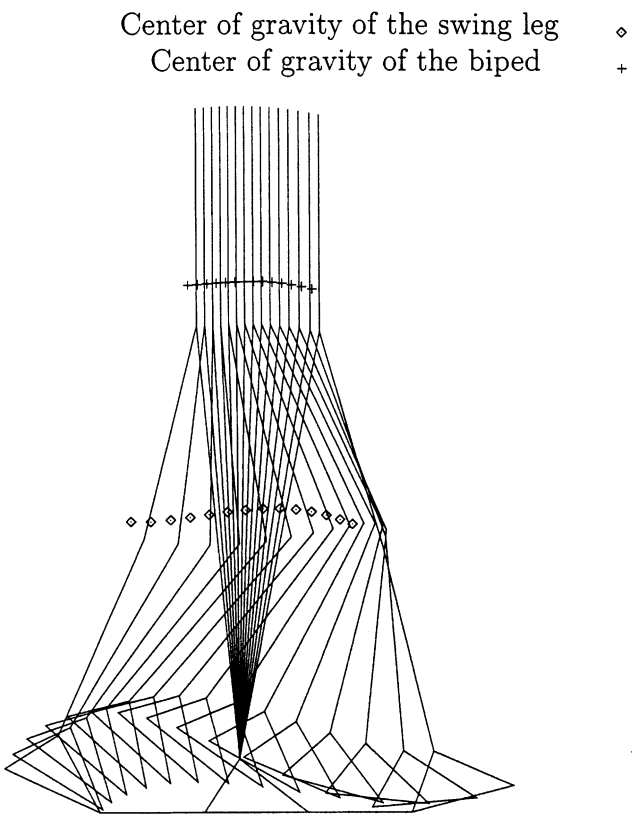


Fig. 14. Example 3: Symmetrical heel-touch with moderate impact.

$$\begin{cases} 0 < \alpha_i < 1 \\ 0 < a_i < r_i \\ -r_i < b_i < r_i \end{cases}, \quad \text{with} \begin{cases} r_2 = 0.41\ (m) \\ r_3 = 0.4\ (m) \\ r_4 = 0.165\ (m) \\ r_5 = 0.41\ (m) \end{cases} \tag{26}$$

Although theoretically acceptable, such bounds are not very realistic. But, in this way, we give maximum freedom to the minimization problem in order that all the constraints can be satisfied at best with reduced impact velocity.

Figure 17 shows the movement generated on the basis of data (26). All initial and final constraints, as well as permanent constraints are respected. The biped reaches the symmetrical point without impact velocity (see Table IV). But the step pattern is not natural.

Furthermore, the comparison between data of Tables V and VI shows that the centres of inertia are strongly shifted backwards with respect to the segmentary axes (see also Figure 17).

This result represents the new balance of inertia required to achieve an impactless heel-touch. But, as shown in Table V, the corresponding mass distribution is not realistic and is quite removed from the data of the reference model given in

Table III. Example 3: Step computed characteristics

Time	$\dot{q}_1$	$\dot{q}_2$	$\dot{q}_3$	
t^i	−0.83	4.94	−5.16	(rad/s)
t^f	−1.14	−3.42	8.45	(rad/s)
L(m)	T(s)	$\bar{v}$(m/s)	v_x(m/s)	v_y(m/s)
0.4	0.35	0.69	3.8	−0.126

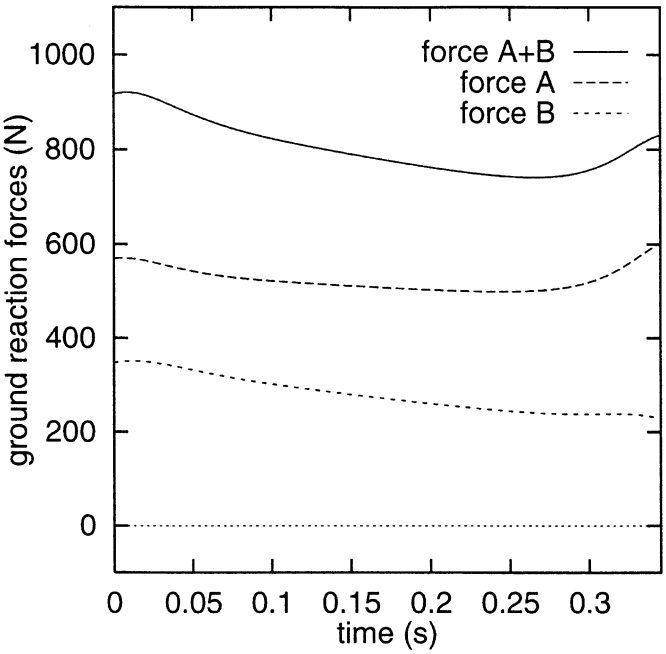


Fig. 15. Example 3: Ground reaction forces.

Table VI. Consequently, the bounds defined in (26) must be decreased.

In the second example, this change is realized as follows

$$i = 2, \ldots, 5, \quad \begin{cases} 0.8 \times \alpha'_i < \alpha_i < 1.2 \times \alpha'_i \\ 0.1 \times r^i < a_i < 0.9 < r_i \\ -\frac{r_i}{2} < b_i < \frac{r_i}{2} \end{cases} \tag{27}$$

where α'_i represents the mass ratio of the ith link of the anthropometric biped BIP with respect to its total mass. The biped motion which results, is shown in Figure 18. The step pattern nearly approaches natural gait.

We may notice that in both previous cases, the algorithm chooses the maximum permitted value for b_5 (see Tables V

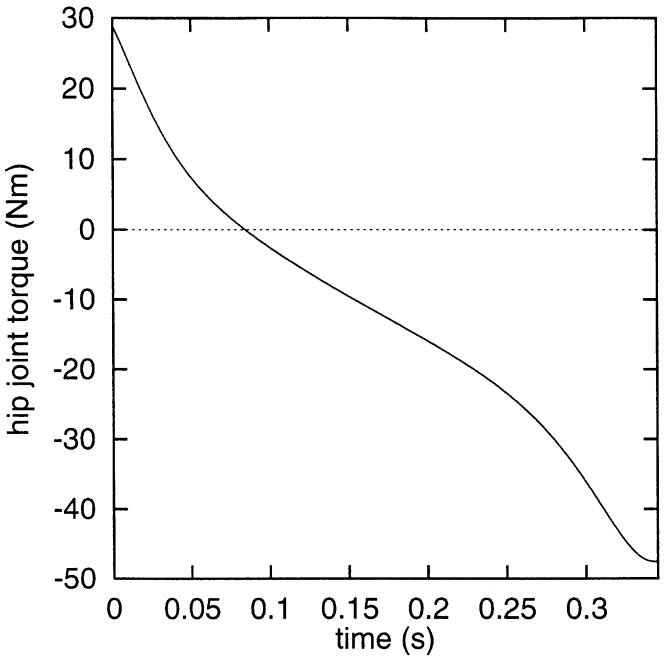


Fig. 16. Example 3: Active torque at hip joint.

https://doi.org/10.1017/S0263574700003027 Published online by Cambridge University Press

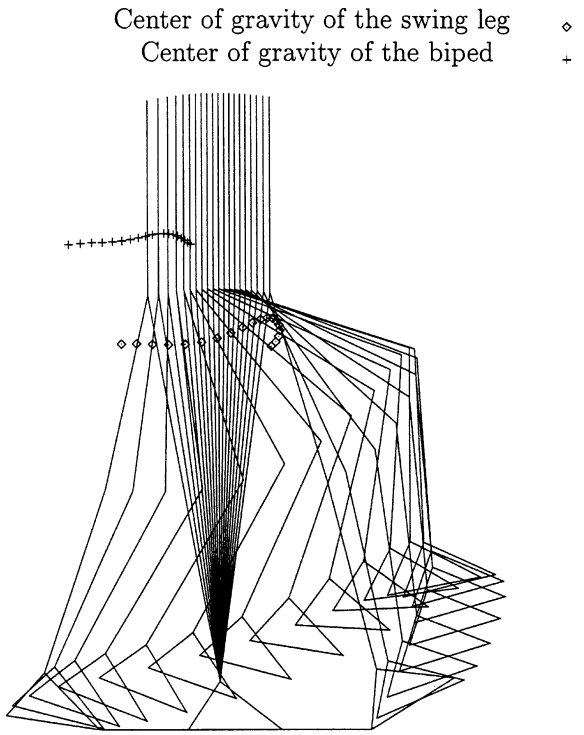


Fig. 17. Example 4: Free mass distribution. Swing motion without super-flexion, and with impactless symmetrical heel-touch.

Table IV. Example 4: Step computed characteristics

Time	$\dot{q}_1$	$\dot{q}_2$	$\dot{q}_3$	
t^i	− 1.24	2.74	− 4.21	(rad/s)
t^f	− 0.68	− 9.16	6.32	(rad/s)
L(m)	T(s)	$\bar{v}$(m/s)	v_x(m/s)	v_y(m/s)
0.39	0.475	0.55	0.0	0.0

Table V. Example 4: Computed mass distribution and centers of mass coordinates.

	L_2	L_3	L_4	L_5
m_i (kg)	25.62	0.75	0.12	34.2
a_i (m)	0.063	0.005	0.115	0.41
b_i (m)	− 0.013	− 0.36	− 0.023	0.41

Table VI. Mass distribution and centers of mass locations of the biped "BIP".

	L_2	L_3	L_4	L_5
m_i (kg)	8.6	6.4	1.09	55.0
a_i (m)	0.14	0.163	0.083	0.329
b_i (m)	0.0	0.0	0.0	0.0
$I^i_{zz}(kgm^2)$	0.232	0.249	0.015	7.0

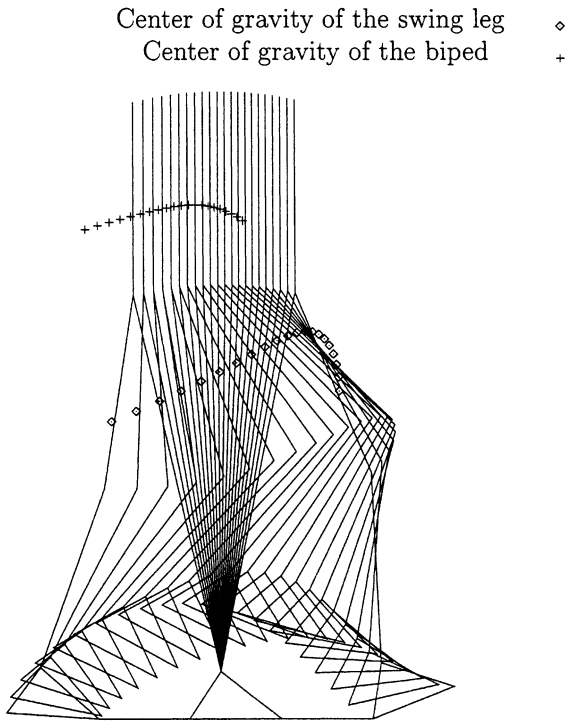


Fig. 18. Example 5: Constrained mass distribution. Swing motion without super-flexion and with moderate impact velocity.

and VII), and for this reason, the center of gravity of the system still remains in a backward position. The link masses (Table VII) remain rather close to their reference values (Table VI). But, we see on Table VIII that a significant impact velocity reappears at heel-touch.

Now, let us examine how the motion can evolve when considering cone-shaped links.

6.3 Result with cone-shaped links

Let us recall that additional parameters c_i, d_i and α_i that can be adjusted or optimized define the geometry and the distribution of mass of the link L'_i for $i = 2, \ldots, 5$ (see subsection 6.2). For the sake of brevity, we present one single result on the basis of the bounds defined as follows

Table VII. Example 5: Mass distribution and centers of mass coordinates.

	L_2	L_3	L_4	L_5
m_i (kg)	9.8	5.7	0.87	54.4
a_i (m)	0.149	0.04	0.106	0.366
$b_i(m)$	0.124	− 0.2	− 0.026	0.205

Table VIII. Example 5: Computed step characteristics

Time	$\dot{q}_1$	$\dot{q}_2$	$\dot{q}_3$	
t^i	− 1.18	4.83	− 5.98	(rad/s)
t^f	− 0.85	− 4.78	5.67	(rad/s)
L(m)	T(s)	$\bar{v}$(m/s)	v_x(m/s)	v_y(m/s)
0.397	0.524	0.67	1.8	− 0.99

https://doi.org/10.1017/S0263574700003027 Published online by Cambridge University Press

$$i=2,\ldots,5,\quad \begin{cases} 0.8\times\alpha'_i<\alpha_i<1.2\times\alpha'_i \\ 0<c_i<\frac{r_i}{2} \\ 0<d_i<\frac{r_i}{2} \end{cases} \tag{28}$$

where r_i and α'_i have the values given in (26) and (27). The motion which results is represented in Figure 19.

It may be compared with the motion shown in Figure 18 which is defined on the basis of the same bounds concerning the mass distribution (see (27) and (28)). This comparison may be extended as well to the motion described in Figure 14 which is relative to the reference model of the biped. The first comparison indicates that the two motions are quite different, the second one (Figure 19) being more satisfactory when considering the step pattern. But, this apparent better kinematics is paid by a much higher impact velocity (see Tables VIII and IX). The second comparison shows that both motions (Figures 19 and 14) have a similar step pattern. The new distribution in Table X is not quite different from its reference counterpart (Table VI). However, one can observe that the center of gravity of the leg is lowered while the moment of inertia of the leg links is increased. This moderate change is sufficient to produce an appreciable improvement of the step kinematics; the step

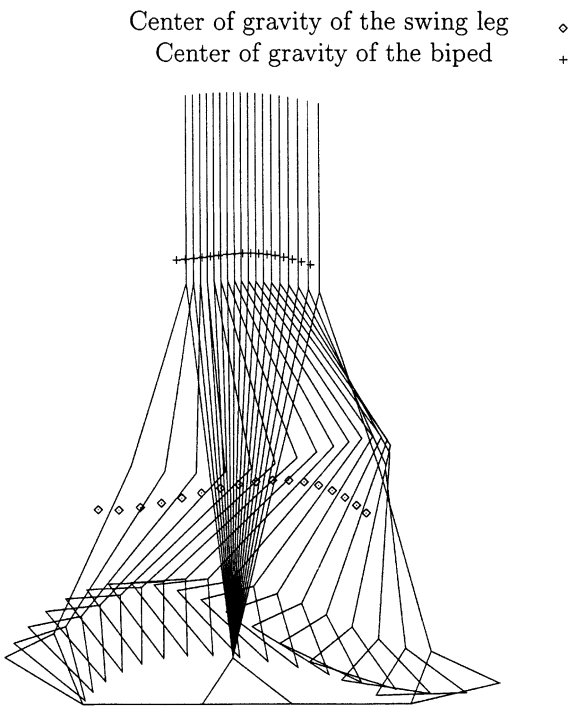


Fig. 19. Example 6: The step lengthens, impact velocity increases.

Table IX. Example 6: Computed step characteristics

Time	$\dot{q}_1$	$\dot{q}_2$	$\dot{q}_3$	
t^i	− 0.85	5.80	− 5.76	(rad/s)
t^f	− 1.29	− 4.91	8.04	(rad/s)
L(m)	T(s)	$\bar{v}$(m/s)	v_x(m/s)	v_y(m/s)
0.465	0.425	0.698	3.0	− 2.07

Table X. Example 6: Mass distribution and moment of inertia of each link.

Link	L_2	L_3	L_4	L_5
$m_i(kg)$	7.72	5.12	1.30	58.9
I^i_{zz} (kgm^2)	0.682	0.522	0.023	6.0

lengthens while the impact velocity decreases (see Tables IX and III), although it remains too high to be realistic.

In Figures 20 and 21 the variations of both ground reaction forces and active torque at hip joint are quite

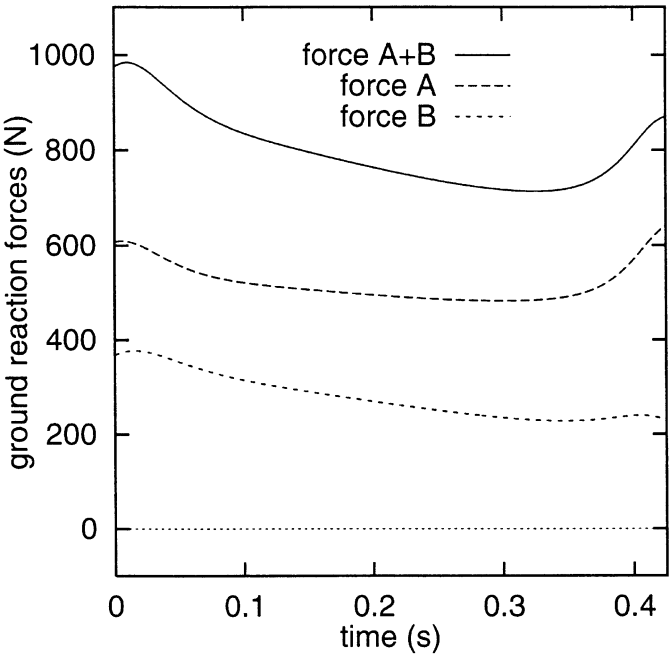


Fig. 20. Example 6: Ground reaction forces.

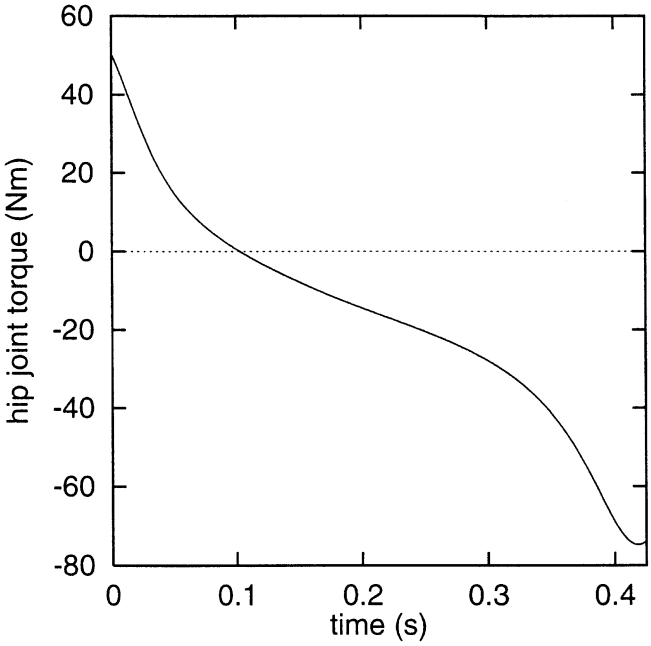


Fig. 21. Example 6: Active torque at hip joint.

https://doi.org/10.1017/S0263574700003027 Published online by Cambridge University Press

similar to their counterparts of Figures 15 and 16, although the torque magnitude is a little greater in the last case.

7. CONCLUSION

An optimization approach has been developed in order to generate and analyze passive swing motions of human-like bipeds. The method presented is based on the minimization of residual values of final constraints as well as on permanent constraints to be respected throughout the motion. The optimizing parameters are the initial postural coordinates together with initial joint velocities which give momentum to the swing motion. Moreover, the optimization process makes it possible to correlate at best the step-length with the swing-time. Numerical simulations are carried out using a full dynamic model of the biped.

The paper is aimed at clarifying the dynamic analysis of motions of bipeds with anthropomorphic locomotion limbs. It offers new means for determining essential features of the gait swing-phase and its suspected pendular or "ballistic" aspect which has been put forward especially in references 6,11,12 and 7.

Numerical results show that the search for purely pendular swings during the unipodal phase of gait is not a realistic issue. But the pendular effect may be favored in order to generate a quasi-conservative swing motion. On the other hand, the computational technique we propose has the ability to adjust the mass distribution of links in order to associate at best the action of gravity with the biped inertia. Such numerical simulations can help to design a biped robot in order to improve its natural dynamic behaviour. Also, let's add that the dynamic analysis method we have presented can be applied to any type of biped able to generate a passive swing.

As a last concluding remark, we can say that fully satisfactory unipodal motions require active control of joints which have been considered as passive during the swing transfer. Generating such controlled motions is the subject of the companion paper (see Part 2: Optimal motion), to appear in the next issue of the journal.

References

1. C.K. Chow & D.H. Jacobson, "Studies of Human Locomotion via optimal Programming," *Mathematical Biosciences* **10**, 239–306 (1971).
2. H. Hatze, "The complete optimization of a human motion," *Mathematical Biosciences* **28**, 99–135 (1976).
3. J. Rose & J.G. Gamble, *Human Walking* (Williams and Wilkins, Baltimore, 1994).
4. T. McGeer, "Passive dynamic walking," *Int. J. Robotics Research* **9**(2), 62–68 (1990).
5. T. McGeer, "Passive walking with knees," *Proceedings of the IEEE International Conference on Robotics and Automation*, Cincinnati, USA, May (1990) pp. 1640–1645.
6. B. Espiau & A. Goswami, "Compass Gait Revisited," *Proc. 4th IFAC Symp. on Robot Control*, Capri, Italy, September (1994) pp. 839–846.
7. A. Goswami, B. Espiau & A. Keramane, "Limit cycles and their stability in a passive bipedal gait," *Proc. 1996 IEEE Int. Conf. Robotics Automation*, Minneapolis, MN (1996) pp. 246–251.
8. J. Pratt & G. Pratt, "Exploiting Natural Dynamics in the Control of a Planar Bipedal Walking Robot," *Proc. of the 36th Annual Allerton Conf. on Communication, Control, and Computing*, pp. 739–748. Monticello, Illinois (1998).
9. J. Pratt & G. Pratt, "Exploiting Natural Dynamics in the Control of a 3D Bipedal Walking Simulation," *Int. Conf. on Climbing and Walking Robots (CLAWAR 99)*, Portsmouth, UK (1999) pp. 797–807.
10. T.A. McMahon, "Mechanics of Locomotion," *Int. J. Robotics Research* **3**(2), 4–28 (1984).
11. S. Mochon & T.A. McMahon, "Ballistic walking: An Improved Model," *Mathematical Biosicences* **52**, 241–260 (1981).
12. S. Mochon & T.A. McMahon, "Ballistic walking," *J. Biomechanics* **13**, 49–57 (1980).
13. Espiau, B. & the BIP team, "BIP: A joint project for the development of an anthropomorphic biped robot," *Proc. 1997 IEEE Int. Conf. on Advanced Robotics*, Monterey, CA-USA (1997) pp. 267–272.
14. P. Sardain, M. Rostami & G. Bessonnet, "An Anthropomorphic Biped Robot: Dynamic Concepts and Technological Design," *IEEE Transactions on Systems Man and Cybernetics* **28**(6), 823–838 (Nov., 1998).
15. P. Sardain, M. Rostami, E. Thomas & G. Bessonnet, "Biped robots: Correlation between technological design and dynamic behavior," *Control Engineering Practice, Journal of IFAC* **7**, 401–411 (1999).
16. B.D. Bunday, *Basic Optimisation Methods* (Edward Arnold, London, 1984).
17. M. Minoux, *Programmation mathématique, théorie et algorithmes* (T. 1 Dunod, 1983).
18. P.E. Gill, W. Murray & M.H. Wright, *Practical Optimization* (Academic Press, London and New York, 1981).
19. R. Flecher, *Practical Methods of Optimization, Constrained Optimization* (John Wiley and Sons, New York and Toronto, 1981), **Vol. 2**.
20. M. Rostami, "Contribution à l'étude dynamique de la phase unipodale de la marche sagittale, et étude du comportement dynamique d'un membre locomoteur anthropomorphe de robot bipède *Thesis* (University of Poitiers, France, March 1999).

Appendix 1

Motion equations of the biped (swing phase)

Following the geometric indications of Figure 2, the dimensional characteristics of the biped can be defined as

$\mathbf{O}_i\mathbf{O}_{i+1} = r_i\mathbf{X}_i$ $i = 1, 2$ (r_i, length of link L_i)

$\mathbf{O}_i\mathbf{G}_i = a_i\mathbf{X}_i$ $i = 1, 2, 4$ (G_i, centre of mass of link L_i)

$\mathbf{O}_3\mathbf{G}_3 = a_3\mathbf{X}_3 + b_3\mathbf{Y}_3$

m_i, mass of link L_i

I_i^{zz}, moment of inertia of L_i about axis $\mathbf{O}_i\mathbf{Z}_0$ ($\mathbf{Z}_0 = \mathbf{X}_0 \times \mathbf{Y}_0$)

Vector of joint coordinates:

$$\mathbf{q} = (q_1, q_2, q_3)^T,\ q_i = (\mathbf{X}_0, \mathbf{X}_i),\ i = 1, 2, 3$$

Symbols

$$C\,ij = cos(q_i - q_j),\ S\,ij = sin(q_i - q_j),\ 1 \le j \le i \le 3$$

T_{14}, torque exerted by L_1 on L_4.

Kinetic energy of the biped

One can write formally

$$T(L_1 \cup \ldots \cup L_4) = \tfrac{1}{2}\,\dot{\mathbf{q}}^T\mathbf{A}(\mathbf{q})\dot{\mathbf{q}}$$

where $\dot{\mathbf{q}} = d\mathbf{q}/dt$, $\mathbf{A}$ is the 3×3 mass matrix such as

https://doi.org/10.1017/S0263574700003027 Published online by Cambridge University Press

$$\mathbf{A} = \begin{pmatrix} A_{11} & A_{12} & A_{13} \\ A_{12} & A_{22} & A_{23} \\ A_{13} & A_{23} & A_{33} \end{pmatrix}$$

with

$$A_{11} = I_1^{zz} + r_1^2(m_2 + m_3 + m_4) \quad A_{12} = r_1(m_2 a_2 C21 + m_3 r_2 C21)$$
$$A_{22} = I_2^{zz} + m_3 r_2^2 \quad A_{13} + m_3 r_1(a_3 C31 - b_3 S31)$$
$$A_{33} = I_3^{zz} \quad A_{23} = m_3 r_2(a_3 C32 - b_3 S32)$$

The q_i-derivatives of $\mathbf{A}$ can be expressed as

$$\mathbf{A}_{,1} = \begin{pmatrix} 0 & E_1 & E_2 \\ E_1 & 0 & 0 \\ E_2 & 0 & 0 \end{pmatrix}, \mathbf{A}_{,2} = \begin{pmatrix} 0 & -E_1 & 0 \\ -E_1 & 0 & E_3 \\ 0 & E_3 & 0 \end{pmatrix}$$

and $\mathbf{A}_{,3} = \begin{pmatrix} 0 & 0 & -E_2 \\ 0 & 0 & -E_3 \\ -E_2 & -E_3 & 0 \end{pmatrix}$

where

$$E_1 = r_1(m_2 a_2 S21 + m_3 r_2 S21)$$
$$E_2 = r_1 m_3(a_3 S31 + b_3 C31)$$
$$E_3 = r_3 m_3(a_3 S32 + b_3 C32)$$

The potential energy is defined as

$$\mathbf{V} = g \sum_i m_i(\mathbf{OG}_i \cdot \mathbf{Y}_0)$$

where the symbol "·" stands for the scalar dot product. Finally, one obtains

$$\mathbf{V} = K_1 S1 + K_2 S2 + g m_3(a_3 S3 + b_3 C3) + g m_4 a_4 S4$$

where

$$K_1 = g\{m_1 a_1 + r_1(m_2 + m_3 + m_4)\}$$
$$K_2 = g(m_2 a_2 + m_3 r_2)$$

Noting $\mathbf{V}_{,i} \equiv \partial \mathbf{V}/\partial q_i$, we have

$$\mathbf{V}_{,1} = K_1 C1$$
$$\mathbf{V}_{,2} = K_2 C2$$
$$\mathbf{V}_{,3} = g m_3(a_3 C3 - b_3 S3)$$

Taking into account the virtual work of the active torque T_{14}, Lagrange's equations of motion can be formulated as

$$\mathcal{L}_i : \frac{d}{dt}\left(\frac{\partial T}{\partial \dot{q}_i}\right) - \frac{\partial T}{\partial q_i} = Q_i \,, I = 1, 2, 3 \qquad (29)$$

with

$$Q_1 = -K_1 C1 - T_{14}$$
$$Q_2 = -K_2 C2$$
$$Q_3 = -\mathbf{V}_{,3}$$

The equation of momentum written in O_2 for L_4, yields the expression of T_{14}:

$$T_{14} = E_4 \ddot{q}_1 + E_5 \dot{q}_1^2 + E_6 \qquad (30)$$

where

$$E_4 = m_4 a_4 r_1 C41 \,,$$
$$E_5 = m_4 a_4 r_1 S41 \,,$$
$$E_6 = m_4 a_4 g C4 \,,$$

with $C41 = cos(q_4 - q_1)$, $S41 = sin(q_4 - q_1)$, $C4 = cos(q_4)$, $q_4 = \alpha = cste$.

Substituting expression (2) for T_{14} in $\mathcal{L}_1$ (cf. 29) one obtains the final formulation of motion equations of the 4-link biped with three free joints. Finally, Lagrange's equations in (29) can be formally written as

$$\mathcal{L}_i(\mathbf{q}, \dot{\mathbf{q}}, \ddot{\mathbf{q}}) = 0 \;, \; i = 1, 2, 3 \qquad (31)$$

Appendix 2

Dimensional characteristics of the biped "BIP" (see Figure 22).

Dimensions of links (see Fig. 2):

$$\vec{O_j O}_{j+1} = r_j \vec{X}_j \;, \; j = 1, \ldots, 5$$
$$(r_1, r_2, r_3, r_4, r_5) = (0.4, 0.41, 0, 0.41, 0.4)(m)$$

Foot dimensions

$$(O_1 A, O_1 B, AB) = (0.12, 0.165, 0.2)(m)$$

Positions of the centers of gravity:

$$\vec{O_i G}_i = a_i \vec{X}_i + b_i \vec{Y}_i \,, \; i = 1, \ldots, 6$$
$$(a_1, a_2, a_3, a_4, a_5, a_6) = (0.24, 0.27, 0.33, 0.14, 0.163, 0.004)(m)$$
$$(b_1, b_2, b_3, b_4, b_5, b_6) = (0, 0, 0, 0, 0, 0.08)(m)$$

Link masses:

$$(m_1, m_2, m_3, m_4, m_5, m_6) = (6.4, 8.6, 55.0, 8.6, 6.4, 1.1)(\text{kg})$$

Moments of inertia of link L_i about O_i

$$(I_1^{zz}, I_2^{zz}, I_3^{zz}, I_4^{zz}, I_5^{zz}, I_6^{zz})$$
$$= (0.44, 0.69, 7.0, 0.23, 0.25, 0.015)(\text{kg.m}^2)$$

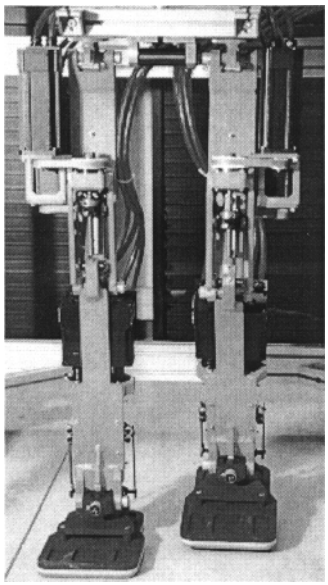


Fig. 22. Example 6: Locomotion system of the biped robot BIP.

https://doi.org/10.1017/S0263574700003027 Published online by Cambridge University Press